Rev. Adv. Mater. Sci. 29 (2011) 142-149

MAGNETIC RESONANCE STUDY OF NANOCRYSTALLINE ZnO NANOPOWDERS DOPED WITH Fe_2O_3 OBTAINED BY HYDROTHERMAL SYNTHESIS

N. Guskos[1,2], J. Typek[2], G. Zolnierkiewicz[2], K. Wardal[2], D. Sibera[3] and U. Narkiewicz[3]

[1]Solid State Section, Department of Physics, University of Athens, Panepistimiopolis, 15 784, Greece
[2]Institute of Physics, West Pomeranian University of Technology, Al. Piastow 48, 70-311 Szczecin, Poland
[3]Institute of Chemical and Environment Engineering, West Pomeranian University of Technology, K. Pulaskiego 10, 70-322 Szczecin, Poland

Received: July 11, 2011

Abstract. Nanoparticles in the $n(Fe_2O_3)/(1-n)ZnO$ system (where the composition index n=0.05, 0.10, 0.20, 0.30, 0.40, 0.50, 0.60, and 0.70) were prepared by using a microwave assisted hydrothermal method. According to XRD analysis the main phase was $ZnFe_2O_4$. The ferromagnetic resonance (FMR) investigation of the obtained samples has been carried out at room temperature. An almost symmetrical and very intense magnetic resonance line centred near g = 2.0 was recorded in all samples. The integrated intensity of lines increased with the ferrite content, reaching a maximum for n = 0.70. The magnetic resonance study has shown that the magnetic resonance line originates from magnetic nanoparticles $ZnFe_2O_4$ and strongly depends on the concentration of the ferrite spinel. The magnetic resonance results have been compared with a similar study of samples the same system but obtained using a high temperature treatment in a classical coprecipitation-calcination synthesis. The analysis of the magnetic resonance data has shown that the concentration of $ZnFe_2O_4$ was smaller in samples obtained by the hydrothermal method and this is consistent with XRD results.

1. INTRODUCTION

Doped ZnO with a relatively large direct band gap of 3.3 eV at room temperature is a very important material in spintronics and is widely used in optoelectronic devices [1-4]. Zinc oxide doped with transition metal ions could be ferromagnetic at room temperature and it belongs to the class of materials called diluted magnetic semiconductors [5-8]. However, the origin of ferromagnetic state is not very well understood. More experimental data are needed to decide whether the magnetic state arises from the magnetic ions substituting in the ZnO lattice or from the secondary magnetic phases and metal precipitates [9-13]. The ferromagnetism could be formed by inclusions of nanoscale oxides of transitions metals (or nanoparticles containing a large concentration of magnetic ions). It was shown that nanosize superparamagnetic precipitates can be responsible for a ferromagnetic-like response at room temperature [14].

Recently, ZnO nanopowders doped with iron oxide synthesized by two methods: coprecipitation-calcination and hydrothermal have been characterized by XRD, Raman and magnetic methods [15-19]. The nanocrystalline samples of ZnO doped with Fe_2O_3 contain crystalline phases of $ZnFe_2O_4$, γ-Fe_2O_3, and ZnO [15]. In a given sample prepared using hydrothermal synthesis the amount of $ZnFe_2O_4$ ferrite spinel phase is lower in comparison

Corresponding author: J. Typek, e-mail: typjan@zut.edu.pl

with the same sample synthesized by calcination method [16-19]. The mean crystallite size of $ZnFe_2O_4$ varies from 8 to 12 nm with increase of γ-Fe_2O_3 content. The degree of agglomeration of nanopowders depends on the amount of Fe_2O_3 and decreases with increasing iron oxide content. The Mossbauer spectra and magnetic measurements at various temperatures have shown that the T_N could change for the bulk $ZnFe_2O_4$ ferrite from 9K up to above 77K which could be attributed primarily to the redistribution of Fe and Zn cations on the A and B sites depending on the preparation technique [20-23]. Usually the $ZnFe_2O_4$ spinel ferrite is paramagnetic at room temperature.

Recently, the magnetic resonance technique investigation of fine particles from the $n(Fe_2O_3)$/(1-n)ZnO system (n = 0.05 to 0.7) prepared by the calcination method has been carried out at room temperature [24,25]. An almost symmetrical and very intense magnetic resonance line was recorded for all samples. The resonance line was centred near g = 2.0 and its integrated intensity increased with ferrite content, reaching the maximum value for n = 0.70. The exchange narrowing effect was observed, especially for sample with n = 0.7 where the phase of ferrite spinel coexisted with the ferromagnetic γ-Fe_2O_3.

In this report we describe ferromagnetic resonance (FMR) study at room temperature of fine particles from the $n(Fe_2O_3)$/(1-n)ZnO system (for n = 0.05, 0.10, 0.20, 0.30, 0.40, 0.50, 0.60, and 0.70) prepared by the hydrothermal method. Comparison of the obtained results will be made with a related investigation of similar samples obtained in the coprecipitation-calcination synthesis.

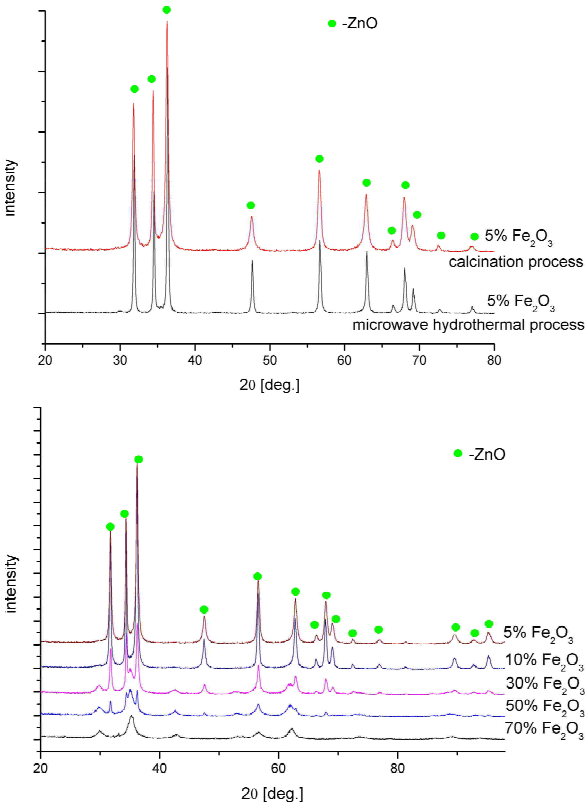

Fig. 1. (a) Comparison of XRD patterns of $n(Fe_2O_3)$/(1-n)ZnO nanopowders (for n = 0.05) obtained in by the coprecipitation-calcination and hydrothermal methods. (b) XRD patterns of ZnO doped by Fe_2O_3 in microwave hydrothermal process. Peaks attributed to ZnO are marked as *, not marked peaks are attributed to $ZnFe_2O_4$

2. EXPERIMENTAL

A mixture of iron and zinc hydroxides was obtained by addition of 2 M solution of KOH to a 20% solution of a proper amount of $Zn(NO_3)_2 \cdot 6H_2O$ and $Fe(NO_3)_3 \cdot 4H_2O$ in water. The obtained hydroxides were put in the reactor with microwave emission. The microwave assisted synthesis was conducted under a pressure of 3.8 MPa for 15 min. The obtained product was filtered and dried.

The phase composition of samples was determined using X-ray diffraction (XRD) (Cu K_α radiation, X'Pert Philips). The mean crystallite size of the detected phases was determined using the Scherrer's formula. The specific surface area of the nanopowders was determined by the Brunauer–Emmett–Teller (BET) method using the equipment Gemini 2360 of Micromeritics. The helium pycnometer AccuPyc 1330 of Micromeritics was applied to determine the density of powders. The morphology of samples was investigated using scanning electron microscopy (LEO 1530 and Zeiss Supra).

The measurements of magnetic resonance spectra were performed on conventional X-band (ν = 9.4 GHz) Bruker E 500 spectrometer with 100 kHz magnetic field modulation. Samples containing around 20 mg of powder were placed in 4 mm diameter quartz tubes. The measurements were carried out at room temperature.

3. RESULTS AND DISCUSSION

Fig. 1a shows the XRD patterns of ZnO doped with 5% Fe_2O_3 obtained by two different methods of preparation (hydrothermal and calcinations processes). The ZnO phase dominates in both cases. The contents of $ZnFe_2O_4$ phase increases with decreasing concentration of ZnO phase for

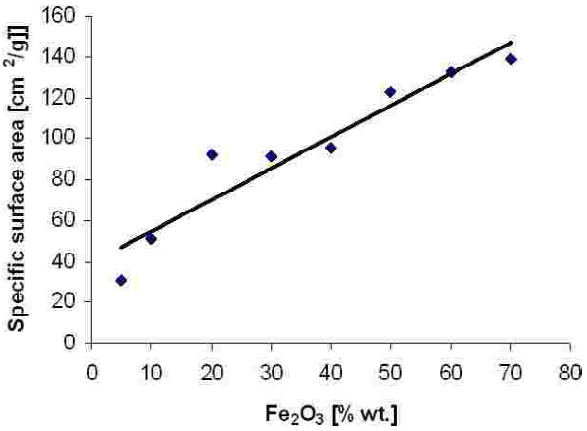

Fig. 2. Dependence of the specific surface area on the concentration of the Fe_2O_3 component.

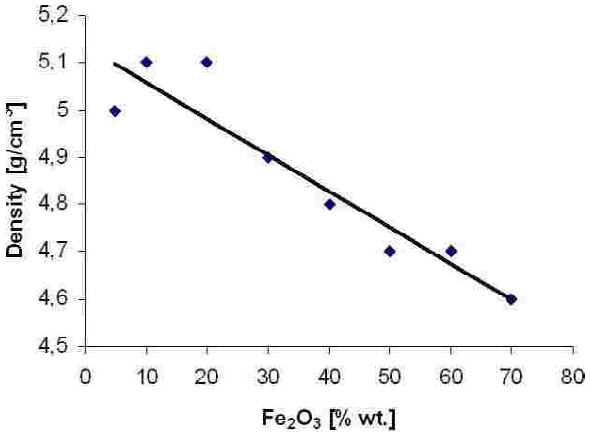

Fig. 3. Dependence of the density on the concentration of the Fe_2O_3 component.

higher values of *n* (Fig.1b). For the overall range of composition index *n* the phases of ZnO and $ZnFe_2O_4$ can be detected using XRD [16]. The intensity of peaks corresponding to the ferrite spinel increases with increasing Fe_2O_3 content. The XRD pattern shows that up to *n*=0.20 only one ZnO phase is recorded, however the shape of the peaks is not symmetric which suggested that some small amount of ferrite spinel phase could be also present. The mean crystallite size of $ZnFe_2O_4$ varies from 8 to 12 nm. In samples obtained by the hydrothermal process the amount of the ferrite spinel phase is lower in comparison with samples obtained by the calcination process. In the XRD spectrum of the *n*=0.5 sample obtained in the hydrothermal process the XRD peaks attributed to ZnO phase are visible, whereas in the case of samples synthesized by the calcination method they are much less evident. Despite the differences in the phase composition, the samples obtained in microwave reactor had considerably larger specific surfaces and smaller density comparing with the samples obtained in the calcination process.

Figs. 2 and 3 present the results of the specific surface area and density measurements. The increase of Fe_2O_3 concentration in samples causes a drop of density and an increase of specific surface area. It is also illustrated by the SEM images showing the morphology of obtained samples (Fig. 4). The powders containing more iron oxide are less agglomerated than samples with a lower content of Fe_2O_3. The samples obtained in microwave reactor had considerably larger specific surface area and smaller density compared with the samples obtained in calcination process. A smaller density in comparison to the calcinated material is connected with a finer grain size [16]. The surface layer of hydroxides may contribute to lower density, the presence of a considerable amount of OH groups on the surface of hydrothermally synthesized powders can be assumed. During this preparation procedure small amounts of Fe_3O_4 or $Fe_{1-x}O$ phases could appear [26,27]. These phases could produce magnetic resonance spectra but from XRD and SEM measurements it is known that the samples are dominated by two magnetic phases: γ-Fe_2O_3 and $ZnFe_2O_4$.

Fig. 5 presents the magnetic resonance spectra in a first derivative mode of a series of *n*(Fe_2O_3)/(1-*n*)ZnO samples obtained by the hydrothermal process with the composition index ranging from $n = 0.05$ to 0.70. The magnetic resonance spectra are dominated by slightly asymmetrical and very intense, broad line similar as for samples obtained by the calcination method. The registered spectra are typical for magnetic nanoparticles in a superparamagnetic phase [28,29]. The intensity of FMR spectra increases with the composition index *n* what suggests that the spectra could be attributed to $ZnFe_2O_4$ nanoparticles. For description of magnetic resonance spectrum of this type a few different relevant lineshapes have been considered [30]. The obtained spectra of *n*(Fe_2O_3)/(1-*n*)ZnO samples have been fitted by the Landau-Lifshitz-shape line. In case of the linear polarization of the microwave field and for a perfect ferromagnet the following equation for the absorption Landau-Lifshitz lineshape could be used [30]:

$$I(H) = \frac{C \times H_r^2 \left[\left(H_r^2 + \Delta_H^2 \right) H^2 + H_r^4 \right] \Delta_H}{\left[H_r^2 \left(H - H_r \right)^2 + H^2 \Delta_H^2 \right] \left[H_r^2 \left(H + H_r \right)^2 + H^2 \Delta_r^2 \right]},$$

where *C* is a numerical constant, H_r is the intrinsic resonance field, and Δ_H is the intrinsic linewidth.

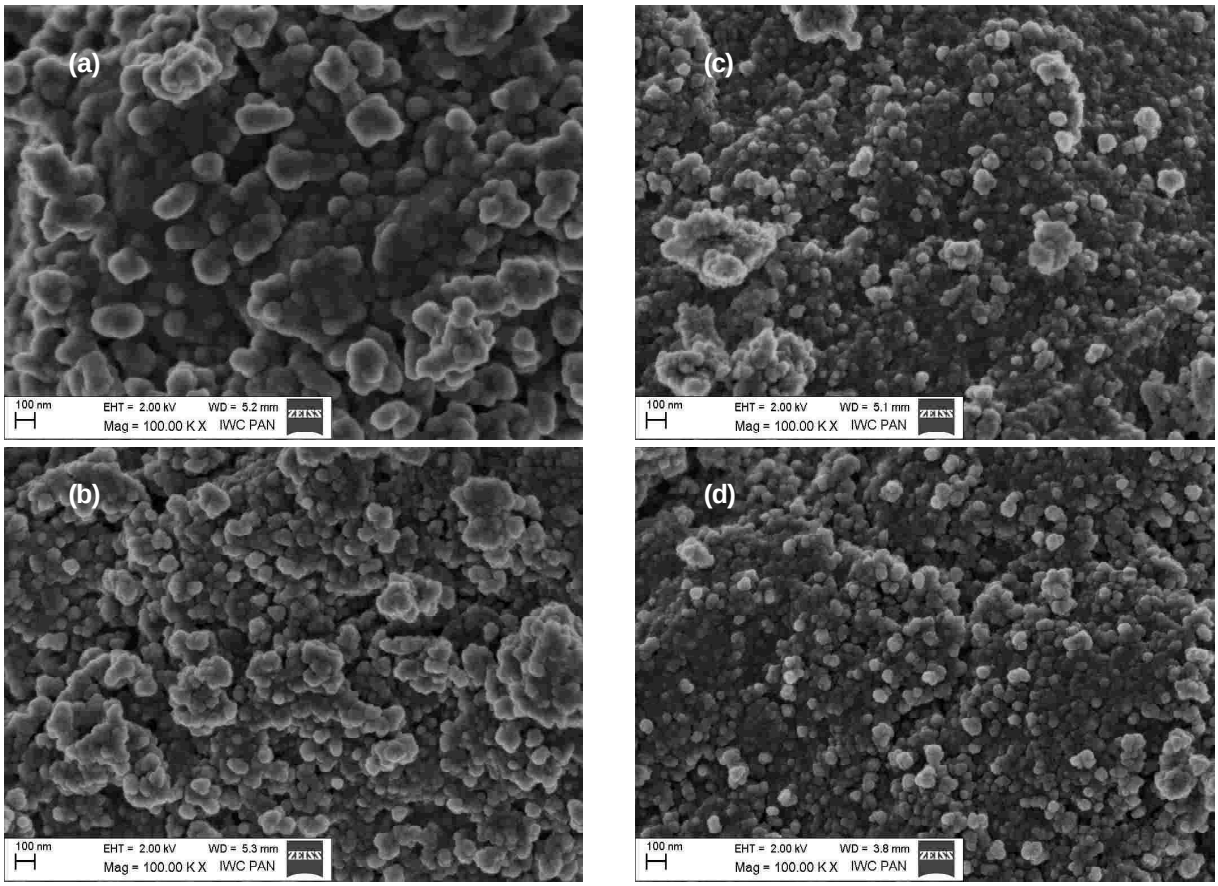

Fig. 4. SEM images of $n(Fe_2O_3)/(1-n)ZnO$ nanopowders obtained in the hydrothermal method: (a) $n = 0.20$; (b) $n = 0.40$; (c) $n = 0.60$; (d) $n = 0.70$.

The fitting of the FMR spectra with a single Landau-Lifshitz-shape line was very sucessful for all samples except for the sample with the composition index $n = 0.70$ (Fig. 6). It was found that fitting with two Landau-Lifshitz lines significantly improves the final result for that $n = 0.70$ sample. This is to be expected as in that sample the amount of ZnO might be to small to incorporate the whole Fe_2O_3 component and, as a results, a small amount of Fe_2O_3 remains in the form of separate iron oxide nanoparticles. If the area under the absorption magnetic resonance line is taken to be proportional to the number of a specific type of nanoparticles than in $n = 0.70$ sample the ratio of numbers of $Fe_2O_3/ZnFe_2O_4$ nanoparticles is close to 0.10.

Essential differences in magnetic response are recorded in comparison with samples obtained by the calcination process (see Fig. 7). In both cases the FMR spectra are due to the aggregated $ZnFe_2O_4$ nanoparticles, but the concentration and the degree of aggregation of magnetic nanoparticles is different. Similar differences in FMR spectra due to the concentration and aggregation differences were previously observed in other magnetic nanosystems [31-34].

In Fig. 8 the peak-to-peak amplitude, the resonance field H_r, and linewidth Δ_H (calculated from the fittings) as a function of the composition index n is given. Because for sample $n = 0.70$ no satisfactory fitting with a single line was achieved, it is not

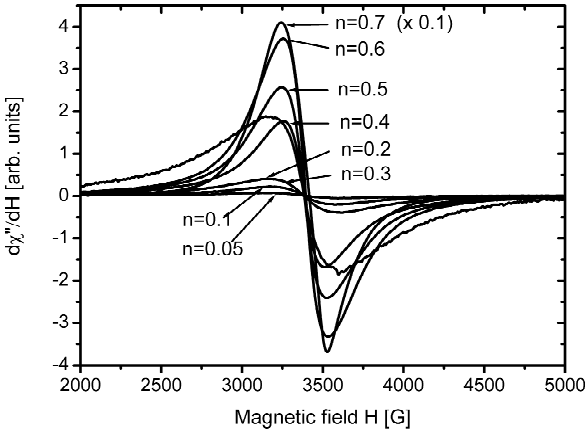

Fig. 5. Room temperature FMR spectra of $n(Fe_2O_3)/(1-n)ZnO$ nanopowders obtained by hydrothermal method. The value of the composition index n is given for each sample.

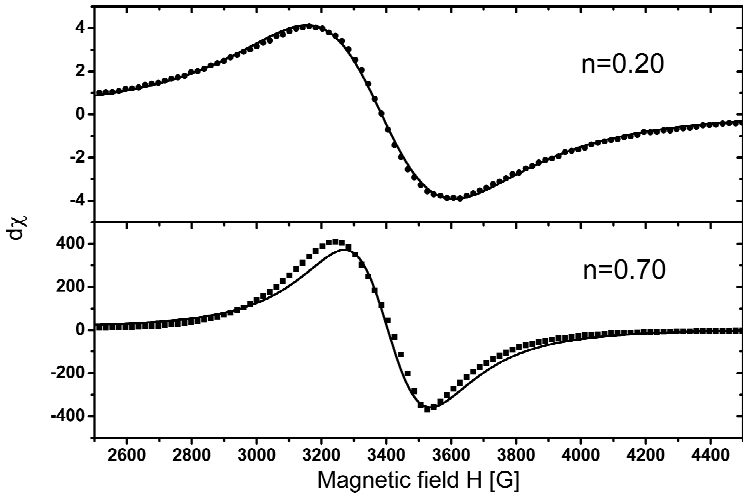

Fig. 6. Fitting of experimental spectra (dots) by a single Landau-Lifshitz-shape line (continuous line) for samples with n = 0.20 (top panel) and n = 0.70 (bottom panel).

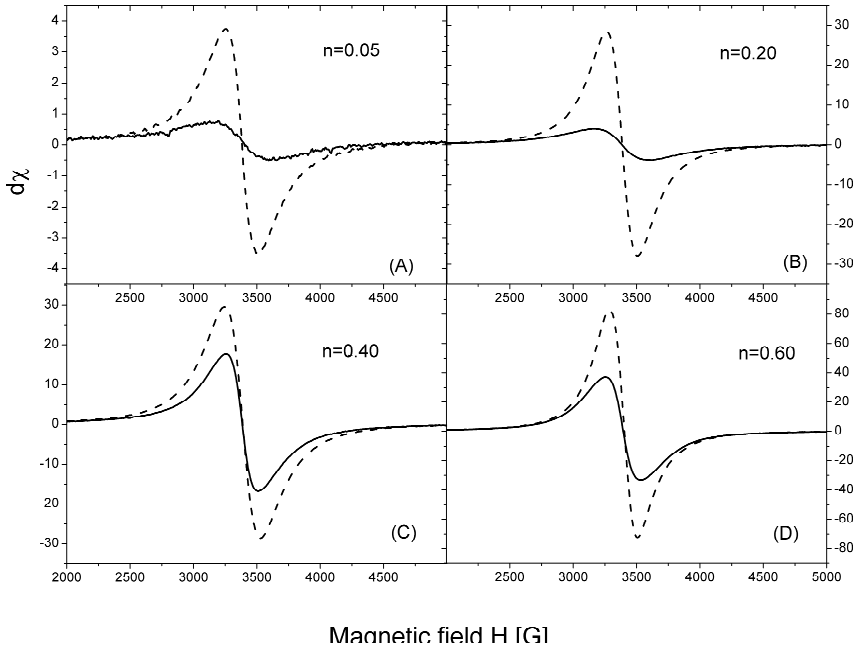

Fig. 7. Comparison of the FMR spectra of $n(Fe_2O_3)/(1-n)ZnO$ nanopowders obtained by the coprecipitation-calcination (continuous line) and hydrothermal (dashed line) synthesis: (A) n = 0.60, (B) n = 0.40, (C) n = 0.20, (D) n = 0.05.

presented in Fig. 8. As expected, the line amplitude increases with the concentration of $ZnFe_2O_4$ nanoparticles for both types of samples and for the same composition index the hydrothermal samples have smaller concentration of $ZnFe_2O_4$. The resonance field of the hydrothermal samples is bigger than for the other ones. This may be connected with the bigger agglomeration of $ZnFe_2O_4$ nanoparticles in the hydrothermal samples. The resonance field of hydrothermal samples does not depend on the composition index, while it increases slowly with the composition index for samples obtained by the calcination process.

The dependence of the linewidth on the composition index for samples obtained by the two different methods is very interesting (Fig. 8, bottom panel). In samples containing small amounts of the $ZnFe_2O_4$ phase (n < 0.40) significant differences in the values of the linewidth are recorded for samples prepared by the two different methods. The broadening of FMR line is more significant for samples obtained by the hydrotermal method for small values of n. In contrast, for samples with n = 0.40, similar linewidths are registered. For higher values of the composition index (n > 0.40) the linewidths of both types of sample are roughly the

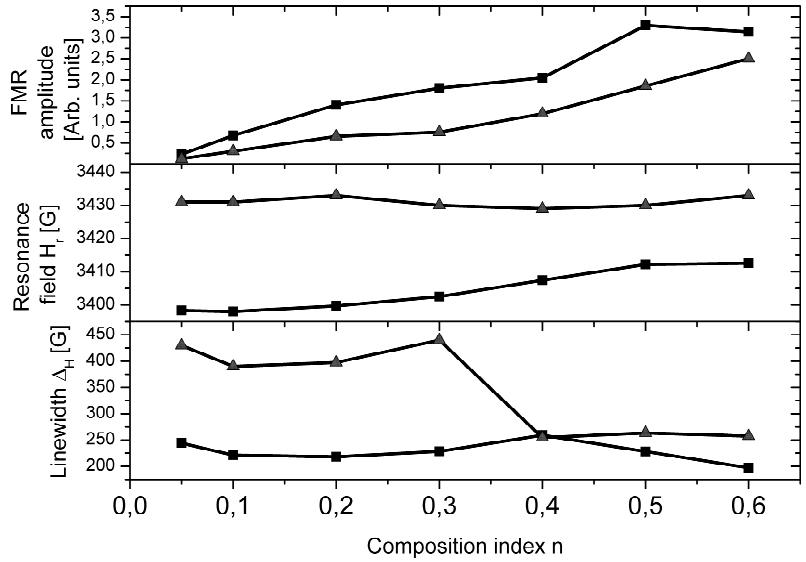

Fig. 8. Dependence of the FMR parameters of $n(Fe_2O_3)/(1-n)ZnO$ nanopowders obtained by the coprecipitation-calcination (squares) and hydrothermal (triangles) synthesis for different values of the composition index *n*: signal amplitude (upper panel), resonance field (middle panel), and linewidth (bottom panel).

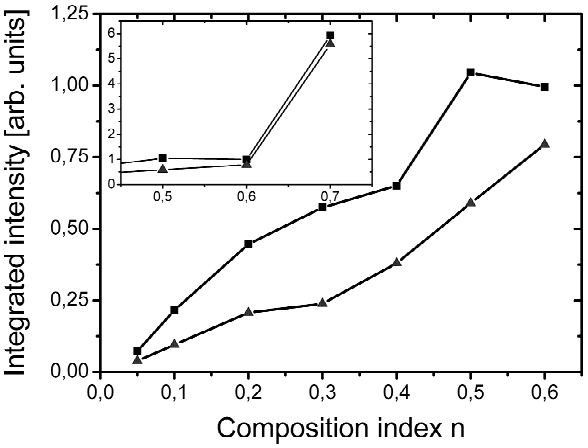

Fig. 9. Dependence of the FMR integrated intensity of $n(Fe_2O_3)/(1-n)ZnO$ nanopowders obtained by the coprecipitation-calcination (squares) and hydrothermal (triangles) synthesis for different values of the composition index *n.* The inset presents (in an extended scale) samples producing the most intense FMR signals.

same. It might be assumed that the exchange narrowing process is responsible for the values of the linewidths. Probably a smaller concentration of $ZnFe_2O_4$ phase (for samples with $n < 0.40$) and different morphology of samples prepared by the hydrothermal process could be the reason of a weaker exchange narrowing for that range of the composition index. The relaxation processes connected with the energy transfer after excitation by the microwave radiation depend strongly on the type of matrix as well as on the concentration of magnetic ions. The broadening of the resonance line of the correlated spin system for sample $n = 0.70$ obtained by the calcinations method could be explained by the coexistence of the ferrous spinel and the iron oxide phases [25].

In Fig. 9 the integrated intensity (calculated as the area under the absorption curve) dependence on the composition index *n* for both types of samples is presented. FMR integrated intensity increases significantly with the increase of the $ZnFe_2O_4$ phase concentration. The same tendency was observed for samples obtained by the calcination method. The integrated intensity could, after scaling, enable calculation of spin concentration. From the XRD measurements is very difficult to estimate a very low concentration of ferrite spinel phase, especially for samples with $n < 0.20$ [15]. The magnetic resonance measurements have shown that a very small concentration of that phase could be easily detected by this technique. The amount of the $ZnFe_2O_4$ phase in samples obtained by the hydrothermal process is roughly two times lower than in samples obtained by calcination method. In both cases the greatest concentration of $ZnFe_2O_4$ phase is seen in samples with the composition index $n = 0.70$.

4. CONCLUSIONS

The FMR spectra of samples from the $n(Fe_2O_3)/(1-n)ZnO$ system are arising from the correlated spin system of the $ZnFe_2O_4$ phase and strongly depend

on sample preparation method. It has been proved that the content of $ZnFe_2O_4$ phase is smaller in hydrothermal samples than in calcined samples with the same value of the composition index. The presence of the $ZnFe_2O_4$ phase has been observed even in samples with small Fe_2O_3 content. In n=0.7 sample the presence of two types of magnetic nanoparticles ($ZnFe_2O_4$ and Fe_2O_3) has been inferred. The degree of agglomeration of nanoparticles has an influence on the FMR parameters of considered nanopowder and thus the magnetic resonance method could be an important technique in characterization of such systems.

REFERENCES

[1] Y. Chen, D.M. Bagnall, H. Koh, K. Park, K. Hiraga, Z. Zhu and T. Yao // *J. Appl. Phys.* **84** (1998) 3912.

[2] J. F. Wager // *Science* **300** (2003) 1245.

[3] S. J. Pearton, D. P. Norton, K. Ip, Y.W. Heo and T. Steiner // *J. Vac. Sci. Technol. B* **22** (2004) 932.

[4] U.Ä. Ozgur, Y. Alivov, C. Liu, A. Teke, M. Reshchikov, S. Dogan, V. Avrutin, S.J. Cho and H. Morko // *J. Appl. Phys.* **98** (2005) 041301.

[5] T. Dietl, H. Ohno, F. Matsukura, J. Cibert and D. Fernand // *Science* **287** (2000) 1019.

[6] J.M.D. Coey, M. Venkatesan and C.B. Fitzgerald // *Nat. Mater*. **4** (2005) 173.

[7] M. Venkatesan, C.B. Fitzgerald, J.G. Lunney and J.M.D. Coey // *Phys. Rev. Lett.* **93** (2004) 177206.

[8] L.M. Huang, A.L. Rosa and R. Ahuja // *Phys. Rev. B* **74** (2006) 075206.

[9] K. Ueda, H. Tabota and T. Kamai L // *Appl. Phys. Lett.* **79** (2001) 988.

[10] S. Kolesnik,B. Dabrowski and J. Mais // *J. Appl. Phys.* **95** (2004) 2582.

[11] G. Lawes, A.S. Risbud, A.P. Ramirez and Ram Seshadri // *Phys. Rev. B.* **71** (2005) 045201.

[12] A. Tomaszewska-Grzeda, A. Opalinska, E. Grzanka, W. Łojkowski, A. Gedanken, M. Godlewski, S. Yatsunenko,V. Osinniy and T. Story // *Appl. Phys. Lett.* **89** (2006) 242102.

[13] C. Sudakar, J.S. Thakur, G. Lawes, R. Naik and V.M. Naik // *Phys. Rev. B* **75** (2007) 054423.

[14] M. Opel, K.-W. Nielsen, S. Bauer, S.T.B. Goennenwein, J. C. Cezar, D. Schmeisser, J. Simon, W. Mader and R. Gross // *Eur. Phys. J. B* **63** (2008) 437.

[15] D. Sibera, R. Jedrzejewski, J. Mizeracki, A. Presz, U. Narkiewicz and W. Lojkowski // *Acta Phys. Pol. A* **116** (2009) S-133.

[16] D. Sibera, U. Narkiewicz, N. Guskos and G. Zołnierkiewicz // *J. Phys: Conference Series* **146** (2009) 012014.

[17] U. Narkiewicz, D. Sibera, I. Kuryliszyn-Kudelska, L. Kilanski, W. Dobrowolski and N. Romcevic // *Acta Phys. Pol. A* **113** (2008) 1695.

[18] N. Romcevic, R. Kostic, B. Hadzic, M. Romcevic, I. Kuryliszyn-Kudelska, W.D. Dobrowolski, U. Narkiewicz and D. Sibera // *J. All. Compd.* **507** (2010) 386.

[19] I. Kuryliszyn-Kudelska, B. Hadzic, D. Sibera, M. Romcevic, N. Romcevic, U. Narkiewicz and W. Dobrowolski // *J. All. Compd.* **509** (2011) 3756.

[20] C. N. Chinnasamy, A. Narayanasamy, N. Ponpandian, K. Chattopadhyay, H. Guerault and J-M Greneche // *J. Phys.: Condens. Matter* **12** (2000) 7795.

[21] F.S. Li, L. Wanga, J.B. Wang, Q.G. Zhou, X.Z. Zhoub, H.P. Kunke and G. Williams // *J. Mag. Mag. Mat.* **268** (2004) 332.

[22] C. Upadhyay, H.C. Vermaa, V. Sathe and A.V. Pimpale // *J. Mag. Mag. Mat.* **312** (2007) 271.

[23] R. De Palma, C. Liu, F. Barbagini, G. Reekmans, K. Bonroy, W. Laureyn, G. Borgh and G. Maes // *J. Phys. Chem. C* **111** (2007) 12227.

[24] N. Guskos, S. Glenis, G. Zolnierkiewicz, J. Typek, D. Sibera, J. Kaszewski, D. Moszyński, W. Łojkowski and U. Narkiewicz // *Physica B* **405** (2010) 4054.

[25] N. Guskos, G. Zolnierkiewicz, J. Typek, D. Sibera and U. Narkiewicz // *Rev. Adv. Mat. Sci.* **23** (2010) 224.

[26] C.T. Liea, P.C. Kuo, W.C. Hsu, I.J. Changa and J. W. Chen // *J. Mag. Mag. Mat*. **239** (2002) 160.

[27] Y. Li, J. Zhao, J. Jiang and J. Han // *Mat. Res. Bull.* **38** (2003) 1393.

[28] N. Guskos, J. Typek, U. Narkiewicz, M. Maryniak and K. Aidinis // *Rev. Adv. Mater. Sci.* **8** (2004) 10.

[29] N. Guskos, J. Typek, T. Bodziony, Z. Roslaniec, U. Narkiewicz, M. Kwiatkowska and M. Maryniak // *Rev. Adv. Mat. Scie.* **12** (2006) 133.

[30] J. Kliava, In: *Magnetic nanoparticles*, ed. by Sergey P. Gubin (Wiley-VCH, 2009), p. 255.
[31] N. Guskos, V. Likodimos, S. Glenis, J. Typek, M. Maryniak, Z. Roslaniec, M. Baran, R. Szymczak, D. Petridis and M. Kwiatkowska // *J. Appl. Phys.* **99** (2006) 084307.
[32] N. Guskos, J. Typek, M. Maryniak, A. Guskos, Z. Roslaniec, D. Petridis and E. Sanderek // *Rev. Adv. Mat. Sci.* **14** (2007) 157.
[33] N. Guskos, M. Maryniak, J. Typek, A. Guskos, R. Szymczak, E. Senderek, Z. Roslaniec, D. Petridis and K. Aidinis // *J. Non-Cryst. Solids.* **354** (2008) 4401.
[34] N. Guskos, G. Zolnierkiewicz, J. Typek, M. Orlowski, A. Guskos, Z. Czech and A. Mickiewicz // *Rev. Adv. Mat. Scie.* **23** (2010) 70.